JOURNAL OF Applied Polymer SCIENCE

Dynamic mechanical properties, crystallization behaviors, and low-temperature performance of polypropylene random copolymer composites

Xiaomeng Wang,[1,2] Xiaogang Yin,[1,2] Lijun Wang,[2] Chun Zhang,[2] Wei Gong,[1,2] Li He[2]

[1]College of Materials and Architectural Engineering, Guizhou Normal University, Guiyang 550025, Guizhou, China

[2]National Engineering Research Center for Compounding and Modification of Polymeric Materials, Guiyang 550014, Guizhou, China

Correspondence to: W. Gong (E-mail: gw20030501@163.com) and L. He (E-mail: prclihe@163.com)

ABSTRACT: In this study, polypropylene random copolymer (PPR) composites were prepared by the addition of either three kinds of thermoplastic rubber (TPR) modifiers (types 2088A, 2095, and 2096) or an ethylene–octene copolymer (POE)/high-density polyethylene (HDPE; 2:1 w/w) blend. Differential scanning calorimetry, wide-angle X-ray diffraction, and dynamic mechanical analysis were used to characterize the crystallization behaviors and dynamic mechanical properties of the PPR composites. The results indicated that PPR/POE/HDPE and PPR/TPR2088A had better comprehensive mechanical properties, especially the low-temperature toughness among all of the samples. The obtained PPR/POE/HDPE blends showed a high toughness and good stiffness in the temperature interval from −10 to 23°C with the addition of only 10 wt % POE/HDPE. When the temperature continued to fall below −10°C, the PPR/TPR2088A composites exhibited a better impact toughness without a loss of too much stiffness. The good low-temperature toughness of those two composites was attributed to both the decrease in the crystallinity and the uniform dispersion, obvious interfacial adhesion, and cavitation ability of POE/HDPE and TPR2088A in the PPR matrix. © 2015 Wiley Periodicals, Inc. J. Appl. Polym. Sci. **2016**, *133*, 42960.

KEYWORDS: composites; copolymers; crystallization; mechanical properties; morphology

Received 5 February 2015; accepted 18 September 2015

DOI: 10.1002/app.42960

INTRODUCTION

Polypropylene random copolymer (PPR) is prepared with the addition of 3–7 wt % ethylene embedded randomly in the propylene matrix. PPR is a widely used matrix component in pipes, daily necessities, packaging materials, automobile parts, furniture, thin films, and other industrial fields for its excellent comprehensive mechanical properties, good processing performance, and relatively low costs.[1,2] However, industrial applications of PPR are greatly hindered because of its insufficient impact toughness, especially at low temperatures. Thus, the toughening of PPR has become a research hotspot in recent years.

Great research efforts have been focused on the toughening of PPR through the addition of inorganic fillers, such as $CaCO_3$,[3,4] SiO_2,[5,6] ZnO,[7] and organophilic montmorillonite.[8,9] In addition, many kinds of β-nucleating agents (β-NAs) have been used to toughen PPR.[3,10–12] Mai *et al.*[3] demonstrated that with the addition of 4.0 wt % nano-$CaCO_3$ and 0.5 wt % β-NA, the impact strength of PPR/nano-$CaCO_3$/β-NA was about 3.6 kJ/m^2 at −10°C, which was higher than the 2.8 kJ/m^2 value of virgin PPR. Through nano-$CaCO_3$/β-NA synergistic modification, the toughness was increased but at the cost of some of the tensile strength. However, the low-temperature impact toughness of PPR still needs to be improved. On the other hand, the processability and mechanical properties of PPR can be enhanced simultaneously by the broadening of the molecular weight (MW) distribution.[13,14] Yu *et al.*[13] found that through the fine broadening of the MW distribution, the tensile strength of PPR obviously increased, but the impact toughness improved slightly. Additionally, blending modification through the addition of elastomers such as ethylene–octene copolymer (POE),[15] styrene–butadiene–styrene triblock copolymer,[16] styrene–hydrogenated butadiene–styrene triblock copolymer,[16] ethylene/styrene interpolymer[17] and so on[2,11,18–20] has been widely investigated. The impact strength of PPR composites has been largely enhanced by the addition of large amounts of elastomers but normally at the cost of other mechanical properties. In addition, recent studies of the low-temperature impact toughness of PPR have mainly been focused on −10 to 23°C. Therefore, it is still necessary to further improve the impact resistance

Table I. Related Parameters of the TPRs

	TPR		
	2088A	2095	2096
MFR (g/10 min)[a]	44	5	28
Hardness	30	55	80
$\bar{M}_w$	278,152	117,806	76,773
$\bar{M}_w/\bar{M}_n$	1.197	1.321	1.207
[PB]/[PS] (wt %/wt %)	75/25	69/31	65/35
T_g (°C)	−90	−72	−67

M_w, weight-average molecular weight; M_n, number-average molecular weight; *PB*, polybutadiene; *PS*, polystyrene.
[a] MFR was tested at 190°C/5 kg.

properties of PPR without affecting the other mechanical properties, especially under ultralow temperatures (−20°C to −30°C). Actually, nowadays, few studies have reported this issue.

In this study, PPR composites were prepared by the addition of three kinds of thermoplastic rubber (TPR) modifiers (2088A, 2095, and 2096) and POE/high-density polyethylene (HDPE) blends, respectively. The influence of different modifiers on the crystallization behaviors of the PPR blends was investigated by differential scanning calorimetry (DSC) and wide-angle X-ray diffraction (WAXD). Meanwhile, the mechanical properties were characterized in the temperature interval from −30 to 23°C, and the toughening mechanism of the PPR composites at room temperature (23°C) and low temperatures (−30 to 0°C) was also studied.

EXPERIMENTAL

Materials

PPR (type RP2400), with a melt flow rate (MFR) of 0.25 g/10 min (230°C, 2.16 kg) and a 3.8 wt % ethylene content, was supplied by Korean Petrochemical Co. TPR modifiers (types 2088A, 2095, and 2096) were supplied by Jia Xinhao Plastic Co. (Shenzhen, China). POE (8200), with about a 25 wt % octene content, a M_W of approximately 39,000, and an MFR of 5.0 g/min (230°C, 2.16 kg), was obtained from Dow Chemical Co. (SCG, Thailand). HDPE (5200B), with an MFR of 0.35 g/10 min (190°C, 2.16 kg), was supplied by Sinopec Yanshan Petrochemical Co. (Beijing, China). The related parameters of TPRs are given in Table I.

Sample Preparation

The melt blending of the PPR composites was performed with a corotating twin-screw extruder (CTE20, Coperion Machinery Co., Nanjing, China) with a rotation speed of 200 rpm. Temperatures along the barrel were increased from 190 to 210°C. Standard specimens were molded with an injection-molding machine (PL860/290, Haitian Machinery Co., Wuxi, China). The molding temperatures were 230, 225, 220, 215, and 210°C, respectively, and the injection pressures were from 55 to 40 MPa with a decrease of 5 MPa. The formula of the PPR composites is exhibited in Table II.

Characterization

DSC. The thermal behaviors of the PPR composites were investigated by a DSC Q10 analyzer (TA Co.). Approximately 5–10-mg samples were rapidly heated from 40 to 250°C and held for 5 min to eliminate their thermal history. We then cooled them to room temperature at a rate of 10°C/min to observe their crystallization behavior. Afterward, the samples were reheated to 250°C at the same rate to record the melting behaviors. The crystallization temperature (T_c), melting temperature (T_m), and melting enthalpy (ΔH_m) were measured. The crystallinity ($X_{C\text{-DSC}}$) of PPR was calculated according to the following equation[9]:

$$X_{C\text{-}DSC}(\%) = \frac{\Delta H_m}{\Delta H_m^0(1-\phi)} \times 100\% \quad (1)$$

where ΔH_m and $\Delta H_m{}^0$ represent the melting enthalpies of the samples and 100% pure crystalline PP (where $\Delta H_m{}^0 = 177$ J/g[21]), respectively, and ϕ is the mass fraction of modifiers in the PPR composites.

WAXD. The WAXD spectra was recorded with a PANalytical X'Pert Pro diffractometer (PANalytical, The Netherlands) in a 2θ range of 10–30° (5°/min). The measurement was performed with a conventional Cu Kα X-ray ($\lambda = 0.154$ nm, reflection mode) under a voltage of 40 kV and a current of 40 mA. The total crystallinity ($X_{C\text{-WAXD}}$) of the samples was calculated with the following equation:

$$X_{C\text{-}WAXD}(\%) = \frac{\Sigma A_{cryst}}{\Sigma A_{cryst} + \Sigma A_{amorp}} \times 100\% \quad (2)$$

where A_{cryst} and A_{amorp} represent the integral intensities of crystalline and amorphous regions, respectively.

The relative amount of β-form crystals (K_β) was evaluated according to the method proposed by Turner-Jones *et al.*[22]

Table II. Formulas of the PPR Composites

		Modifier				
Sample	PPR	2088A	2095	2096	POE/HDPE = 2 : 1 (wt %)	Masterbatch (wt %)
PPR	100	0	0	0	0	2
PPR/TPR2088A	90	10	0	0	0	2
PPR/TPR2095	90	0	10	0	0	2
PPR/TPR2096	90	0	0	10	0	2
PPR/POE/HDPE	90	0	0	0	10	2

Table III. T_c, T_m, ΔH_m, and $X_{C\text{-}DSC}$ Values of the PPR Composites

Sample	T_c (°C)	T_m (°C)	ΔH_m (J/g)	$X_{C\text{-}DSC}$ (%)
PPR	101.06	146.71	67.83	39.10
PPR/TPR2088A	100.91	143.90	56.70	36.40
PPR/TPR2095	101.64	144.40	58.63	37.64
PPR/TPR2096	100.89	144.99	57.98	37.22
PPR/POE/HDPE	107.97	129.45, 144.57	53.03	36.10

$$K_\beta = \frac{I_{\beta(300)}}{I_{\beta(300)} + I_{\alpha(110)} + I_{\alpha(040)} + I_{\alpha(130)}} \times 100\% \quad (3)$$

where $I_{\beta(300)}$ is the intensity of the (300) reflection peak of the hexagonal β-form crystal at $2\theta = 16.0°$ and $I_{\alpha(110)}$, $I_{\alpha(040)}$, and $I_{\alpha(130)}$ are the intensities of the (110), (040), and (130) reflection peaks of the monoclinic α-form crystals at 14.1, 16.8, and 18.6°, respectively.

Therefore, the crystallinities of the β and α forms (X_β and X_α, respectively) were calculated according to the following equations:

$$X_\beta = X_c \times K_\beta \quad (4)$$

$$X_\alpha = X_c - X_\beta \quad (5)$$

Dynamic Mechanical Analysis (DMA). DMA was performed with a DMA Q800 analyzer (TA Co.). The double-cantilever mode was selected, and the measurement was carried out on a rectangular cross-sectional bar of 35 × 10 × 4 mm^3 (Length × Width × Thickness) from −120 to 120°C at a heating rate of 5°C/min and an oscillatory frequency of 1 Hz.

Mechanical Properties. The notched Izod impact strength of the specimens was measured with a ZBC1400-B Izod machine (SANS, MTS) according to ASTM D256-04. When low-temperature tests were carried out, the specimens were first kept in a thermostat at −30, −20, and −10, 0°C for 4 h, respectively, and were then immediately subjected to impact. The tensile testing was carried out at room temperature (23°C) with a SANS universal tensile testing machine (CMT4204, MTS) in accordance with ASTM D638-03.

Scanning Electron Microscopy (SEM). The microscopic phase morphologies and the impact-fractured surfaces (fractured at 23, −10, and −30°C, respectively) of the samples were observed with an SEM instrument (Quanta FEG250, FEI) at an acceleration voltage of 20 kV. Samples were frozen-fractured in liquid nitrogen. To observe the dispersion of the rubber phase, the cryofractured surfaces were first etched in a mixed liquid of 1.5% w/v potassium permanganate, 70 vol % sulfuric acid, and 30 vol % phosphoric acid for 12 h and then etched by xylene at 60°C for 1 h.[11] All of the specimens were sputter-coated with a thin layer of gold before the observations.

RESULTS AND DISCUSSION

Crystallization Behaviors

PPR blends with and without modifiers were investigated by DSC. The corresponding data are presented in Table III. The crystallization curves of the cooling process are shown in Figure 1(a), and the melting curves of the second heating step are shown in Figure 1(b). From Figure 1(a) and Table III, it was found that the addition of POE/HDPE enhanced T_c of PPR from 101.06°C (T_c of virgin PPR) to 107.97°C. On the contrary, the TPR modifiers (types 2088A, 2095, 2096) did not have a distinct influence on T_c. For the PPR/POE/HDPE composites, the obvious increase in T_c may have been due to the flexible polyolefin blocks (octene segments) of POE, and this acted as nuclei of the PPR macromolecule segments.[15] On the other hand, the T_c values of HDPE and PPR were very analogous;[23] blending the two substances interacting with each other could induce and accelerate the crystallization behavior of the blends.

We found that the addition of any of the four different modifiers had a similar decreasing effect on $X_{C\text{-}DSC}$ of PPR, as shown in Table III. However, the PPR/POE/HDPE and PPR/TPR2088A blends exhibited relatively low crystallinities of 36.10 and 36.40%, respectively. This phenomenon was probably because of the addition of elastomers; this increased the amorphous components in the PPR matrix and resulted in more defects in the crystalline structures.[24] This may have decreased the crystallinity

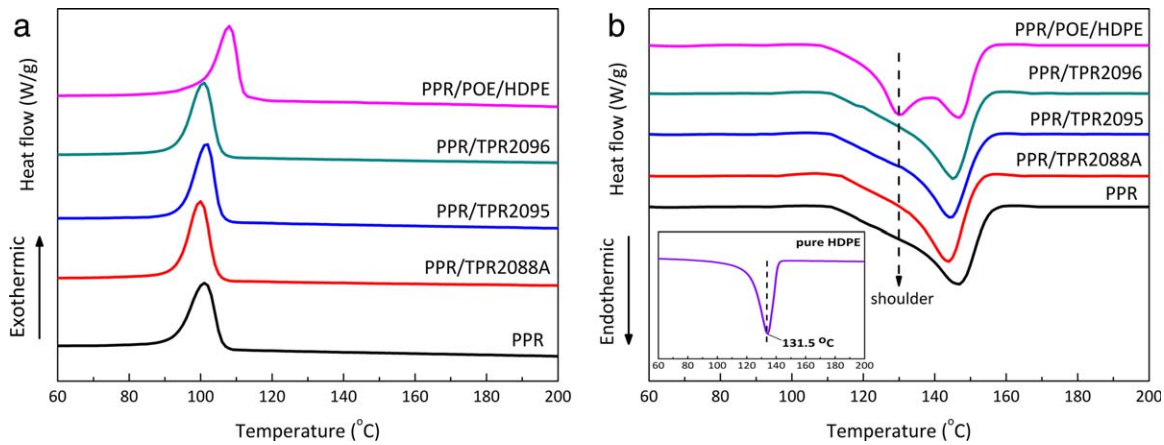

Figure 1. (a) Crystallization and (b) melting curves of the PPR blends. [Color figure can be viewed in the online issue, which is available at wileyonlinelibrary.com.]

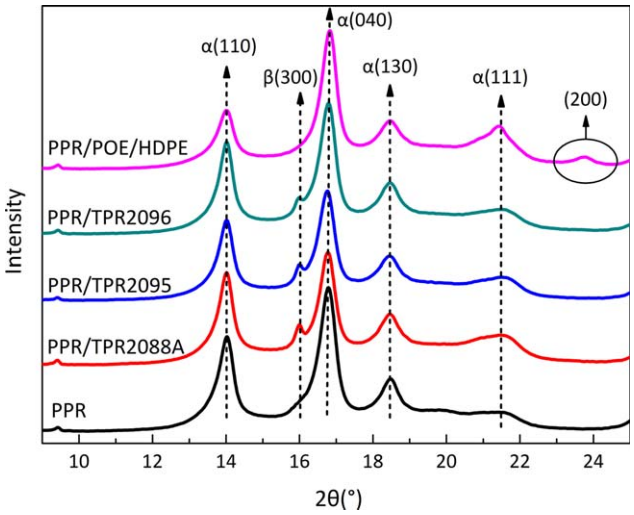

Figure 2. WAXD diffraction patterns of the PPR blends. [Color figure can be viewed in the online issue, which is available at wileyonlinelibrary.com.]

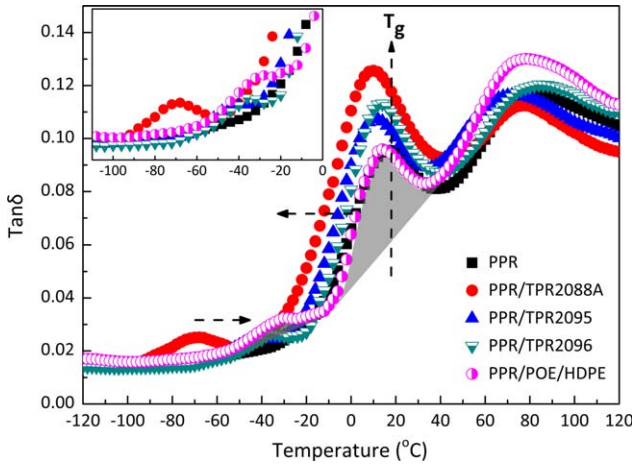

Figure 3. Tan δ values of the PPR blends. [Color figure can be viewed in the online issue, which is available at wileyonlinelibrary.com.]

of the samples and, thus, effectively improved the impact toughness of the materials.

We found that the thermograms of all of the samples showed two peaks [Figure 1(b)]. The peak near 145°C was mainly attributed to the α-crystal melting peak of PPR, and the other shoulder peak appearing near 130°C may have been ascribed to the incomplete crystallization of the PPR matrix. However, an obvious shoulder peak appeared in the curve of the PPR/POE/HDPE blends. This may have been due to the melting peak of HDPE (the melting peak of neat HDPE appeared at 131.5°C); this overlapped with the incomplete crystallization peak of the PPR matrix rather than the generation of a new crystal, which was further confirmed by WAXD. Moreover, as shown in Figure 1(b) and Table III, the addition of modifiers decreased the T_m values of the composites. This was ascribed to the addition of amorphous components, which had a dilution effect on the crystallization region of the PPR matrix.[16]

Figure 2 shows the WAXD diffraction patterns of the PPR blends. The corresponding data are listed in Table IV. For the spectrum of PPR, the most intense reflections were presented at 2θ values of 14.1, 16.8, 18.6, and 21.2° in accordance with the (110), (040), (130), and (111) lattice planes of the most common α crystals. Afterward, for the spectra of PPR/TPR2088A, PPR/TPR2095, and PPR/TPR2096, a new peak at $2\theta = 16.0°$ was observed. This was assigned to the (300) lattice plane of β crystals and indicated the existence of β crystals in the PPR composites. In addition, a new peak at $2\theta = 23.9°$ of PPR/POE/HDPE was found; this corresponded to the characteristic (200) lattice planes of HDPE.[25] This further indicated that the shoulder peak of PPR/POE/HDPE at about 130°C in the DSC test could have been mainly attributed to the melting peak of HDPE [Figure 1(b)]. According to the Turner-Jones report,[22] there may have also existed a (301) reflection of β crystals at 21.2°; this overlaps the (111) reflection of α crystals.[3] Therefore, during the calculation of K_β, intensity, (I) (301), and I (111) were not involved in the analysis.

As shown by Table IV, the $X_{C\text{-}WAXD}$ values of the composites decreased obviously with the addition of modifiers; this was consistent with the results of DSC. Furthermore, the addition of the TPR modifiers (types 2088A, 2095, and 2096) induced the β crystals and made the initiation and propagation of plastic deformation more available and made the absorption of impact energy easier.[26] In addition, K_β of PPR/TPR2088A was 15.5%, which was higher than that of the other samples. The increase of β crystals may have enhanced the energy dissipation and resulted in the improvement of low-temperature impact toughness.

Table IV. $X_{C\text{-}WAXD}$, X_β, X_α, and K_β Values of the PPR Samples

Sample	$X_{C\text{-}WAXD}$ (%)	X_α (%)	X_β (%)	K_β (%)
PPR	62.5	62.5	0	0
PPR/TPR2088A	58.5	49.4	9.1	15.5
PPR/TPR2095	61.6	52.8	8.8	14.3
PPR/TPR2096	60.3	52.5	7.8	12.9
PPR/POE/HDPE	58.9	58.9	0	0

Dynamic Mechanical Properties

The fracture resistance was the essential response of the molecular chain mobility, which could be characterized by DMA. The mechanical loss factors (Tanδ) are shown in Figure 3, and the corresponding data are exhibited in Table V.

Table V. Relaxation Parameters Obtained from the DMA Measurement of the PPR Samples with and without Modifiers

Sample	T_g (°C)	T_e (°C)	$I_{R\text{-}\beta}$	$I_{R\text{-}\alpha}$	I_R
PPR	15.62	—	3.94	—	3.94
PPR/TPR2088A	9.66	−67.95	5.97	1.61	7.58
PPR/TPR2095	11.04	−40.51	4.28	0.69	4.97
PPR/TPR2096	13.61	−36.02	4.37	0.74	5.11
PPR/POE/HDPE	14.07	−30.15	4.03	1.31	5.34

$I_{R\text{-}\beta}$, integration area of the β relaxation of PPR; $I_{R\text{-}\alpha}$, integration area of the α relaxation of the elastomers as revealed by Tanδ.

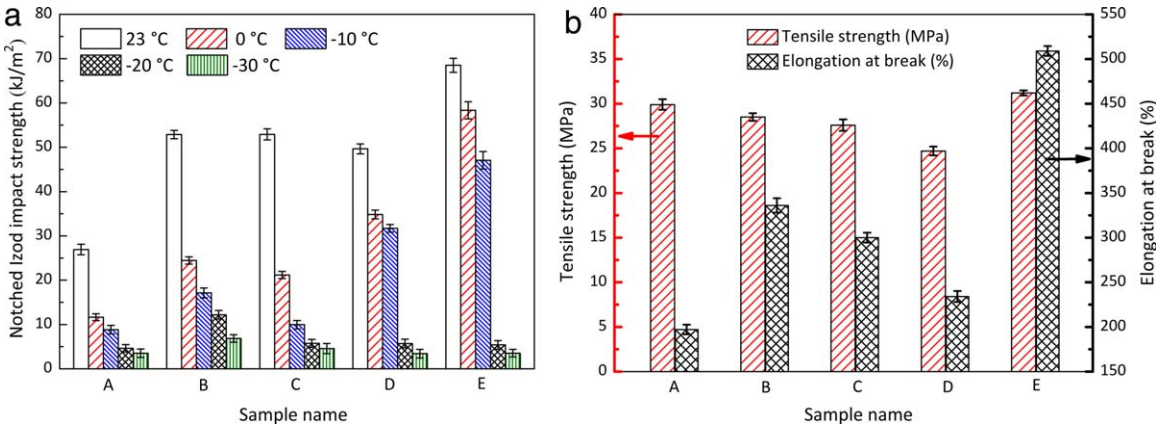

Figure 4. (a) Izod impact strength of the PPR blends obtained at different temperatures and (b) corresponding tensile properties tested at 23°C: (A) PPR, (B) PPR/TPR2088A, (C) PPR/TPR2095, (D) PPR/TPR2096, and (E) PPR/POE/HDPE. [Color figure can be viewed in the online issue, which is available at wileyonlinelibrary.com.]

As shown in Figure 3, we found that all of the curves exhibited three different damping peaks. The first peak at about 80°C was mainly due to the α_c relaxation, and this was related to the relaxation of the restricted molecular chains of PPR in the crystalline phase with defects. It was also known as the rigid fraction.[27–30] The second peak at about 15°C was referred to the β relaxation and was attributed to the glass transition of the unrestricted molecular chains of PPR in the amorphous region. This accounted for the molecular mobility of the matrix. Afterward, the temperature related to the β relaxation peak was defined as the glass-transition temperature (T_g) of the sample.[5,31] In addition, the mechanical loss peaks at low temperatures of −30 to −70°C (T_e) belonged to the α relaxation of TPR or POE of the elastomer-modified PPR. This accounted for the molecular mobility of the elastomer particles.

Obviously, as shown in Figure 3 and Table V, the T_g values of all of the modified samples shifted to lower temperatures when compared with that of the virgin PPR. The T_e values of all of the modified samples translated to higher temperatures compared with the T_g values of the elastomers. To some extent, this partially indicated that the PPR blends showed good compatibility.

In addition, the T_g of PPR/TPR2088A decreased sharply. The reduction in T_g indicated the enhancement of molecular chain mobility in the amorphous region of the PPR composites at a lower temperature. It played a critical role in the low-temperature toughness. In addition, the higher intensity of β relaxation, the more energy dissipation happens. It may lead to higher impact fracture resistance. Although the energy dissipation in the process of viscoelastic relaxation could be responsible for the enhancement of toughness,[10,32] it was not the only factor in determining the toughness.

On the other hand, it was also proven in the reports that there existed a certain relationship between the total integration area of the relaxations (I_R; the β relaxation of PPR together with the α relaxation of elastomers) and the impact strength.[33] Namely, when the sample had an excellent impact strength in the mechanical measurement, it usually showed a bigger I_R during the DMA measurement. This way, the whole relaxation spectrum was taken into account in the material evaluation. So, I_R rather than the maximum of each peak, will always be used to reflect the contributions of all of the structural groups present in the material. The gray shadows depicted in Figure 3 show the areas used to calculate the I_R values of the relaxations. As shown in Table V, the value of I_R of all of the composites was greatly increased in comparison with the virgin PPR. Among them, I_R of PPR/TPR2088A composite improved the most, with an increase of 92.4%, and PPR/POE/HDPE was the second best, with an increase of 35.5%. Moreover, in fact, the α relaxation of the elastomers were first activated under low-temperature impact conditions.[33] As shown in Figure 3, the T_e of PPR/TPR2088A composite was the lowest; this was exactly consistent with its low-temperature performance.

In conclusion, the improvement of the low-temperature toughness of the PPR composites was a common effect of the kinds of factors: the T_g of the matrix and the temperature of the elastomer phase together with I_R.

Mechanical Properties

The results of Izod impact strength, tensile strength, and elongation at break testing of the PPR blends are exhibited in Figure 4.

As shown in Figure 4(a), when the temperature decreased, the impact toughness of each set of the samples showed a trend of decline. However, all of the modified samples exhibited a higher impact strength than that the virgin PPR at five different temperatures. However, the PPR/POE/HDPE blends revealed the best impact strengths at −10 to 23°C among these samples; these were 47.1 kJ/m^2 (−10°C), 58.4 kJ/m^2 (0°C), and 68.5 kJ/m^2 (23°C), respectively. The impact strength of PPR/POE/HDPE was three to five times better than that of the virgin one. This may have been attributed to the POE/HDPE particles, which acted as stress concentration centers in the matrix and may have induced large amounts of shear zones. Therefore, this significantly increased the impact strength of the composites. Moreover, POE not only improved the compatibility of

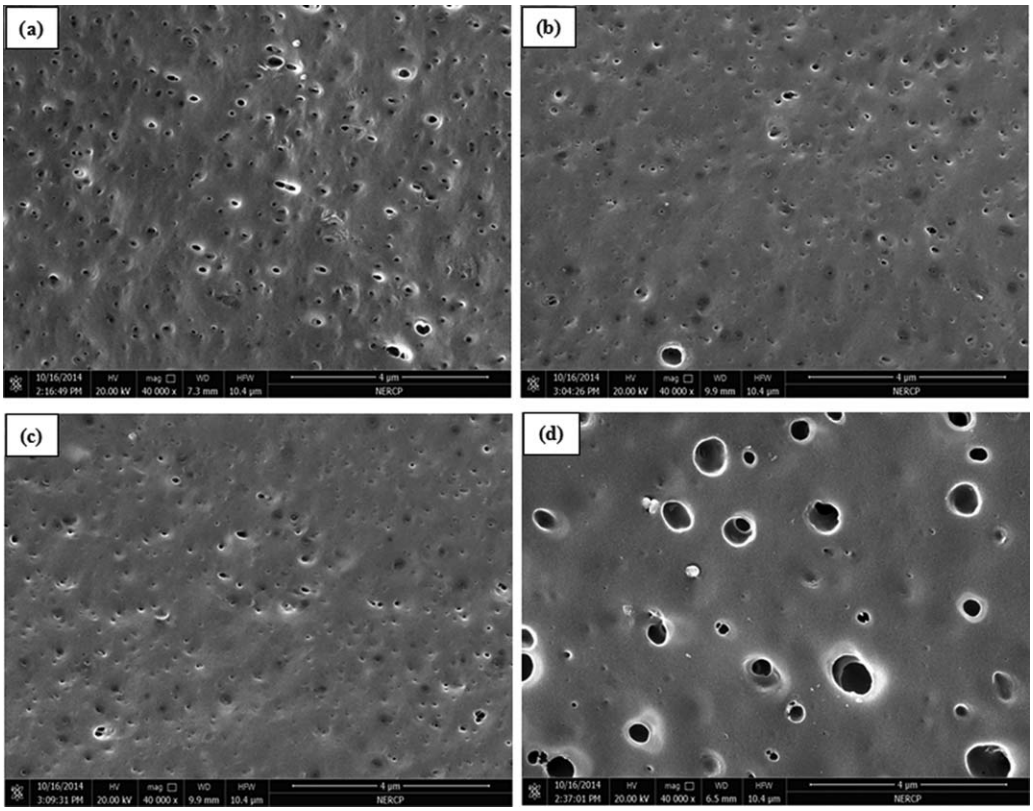

Figure 5. SEM micrographs of the etched samples: (a) PPR/TPR2088A, (b) PPR/TPR2095, (c) PPR/TPR2096, and (d) PPR/POE/HDPE. The scale represents 4 μm.

the PPR/HDPE blends but also blocked and terminated the development of cracks.[24] However, when the temperature continued dropping, the impact strength of PPR/POE/HDPE decreased sharply (5.4 kJ/m^2 at −20°C and 3.5 kJ/m^2 at −30°C), nearly to the value of neat PPR. Meanwhile, the impact toughnesses of PPR/TPR2095 and PPR/TPR2096 were also consistent with that of the neat one at −20 to −30°C. On the contrary, PPR/TPR2088A showed the best toughness among all of these samples at −20 to −30°C, which was twice higher than that of the virgin PPR. The reason may have been the TPR elastomers, which had a similar structure to that of PPR. It could make these two phases generate a transition layer of good miscibility.[34] In addition, the TPR modifiers might also have behaved as a nucleation agent in the PPR matrix;[16] this changed the crystal morphology and refined the PPR spherulites. The small spherulites might have effectively prevented microcracks growth into real cracks[35] and then improved the low-temperature toughness of PPR. On the other hand, the existence of a small amount of high-elastic polybutadiene segments in the composite could accelerate the chain scission and result in proper crosslinking of the PPR matrix;[36] this enhanced the impact and tensile strength of the composite simultaneously. TPR2088A had the lowest hardness, and this reflected the best elasticity. It had a relatively high M_W and high content of polybutadiene (PB) blocks compared with the other two TPR modifiers (the basic differences of the TPR$_s$ are shown in Table I). It tangled with the chain of the matrix easier, and this might have increased the adhesive force between interfaces[37] and improved the impact strength of the composite. As a result, the PPR/TPR blends based on TPR2088A revealed a good impact toughness at ultralow temperatures (−20 to −30°C). However, even when crosslinking or other effects were not present, the presence of an appropriate secondary TPR phase might have increased the toughness of the continuous phase at ultralow temperatures. This is further explained in the Microstructure Morphological Analysis section.

We observed in Figure 4(b) that the tensile strength of the PPR composites presented a downward trend, except for PPR/POE/HDPE. In addition, the tensile strength of PPR/TPR2088A decreased the least among the PPR/TPR composites. The trends of elongation at break were similar to that of the tensile strength.

Consequently, PPR/POE/HDPE obtained good toughness in the temperature interval from −10 to 23°C without a loss in other mechanical properties. In addition, the PPR/TPR2088A blends obtained an obvious enhancement in the toughness, especially at ultralow temperatures (−20°C to −30°C) and at the cost of a slightly lower tensile strength.

Microstructure Morphological Analysis

To investigate the toughening mechanism of the PPR blends, SEM was adopted to inspect the etched microstructures and impact-fractured surfaces of the samples. The typical SEM photographs are shown in Figures 5–8.

As shown in Figure 5, dark holes represented the dispersed phases, which were etched out from the matrix by mixed acid

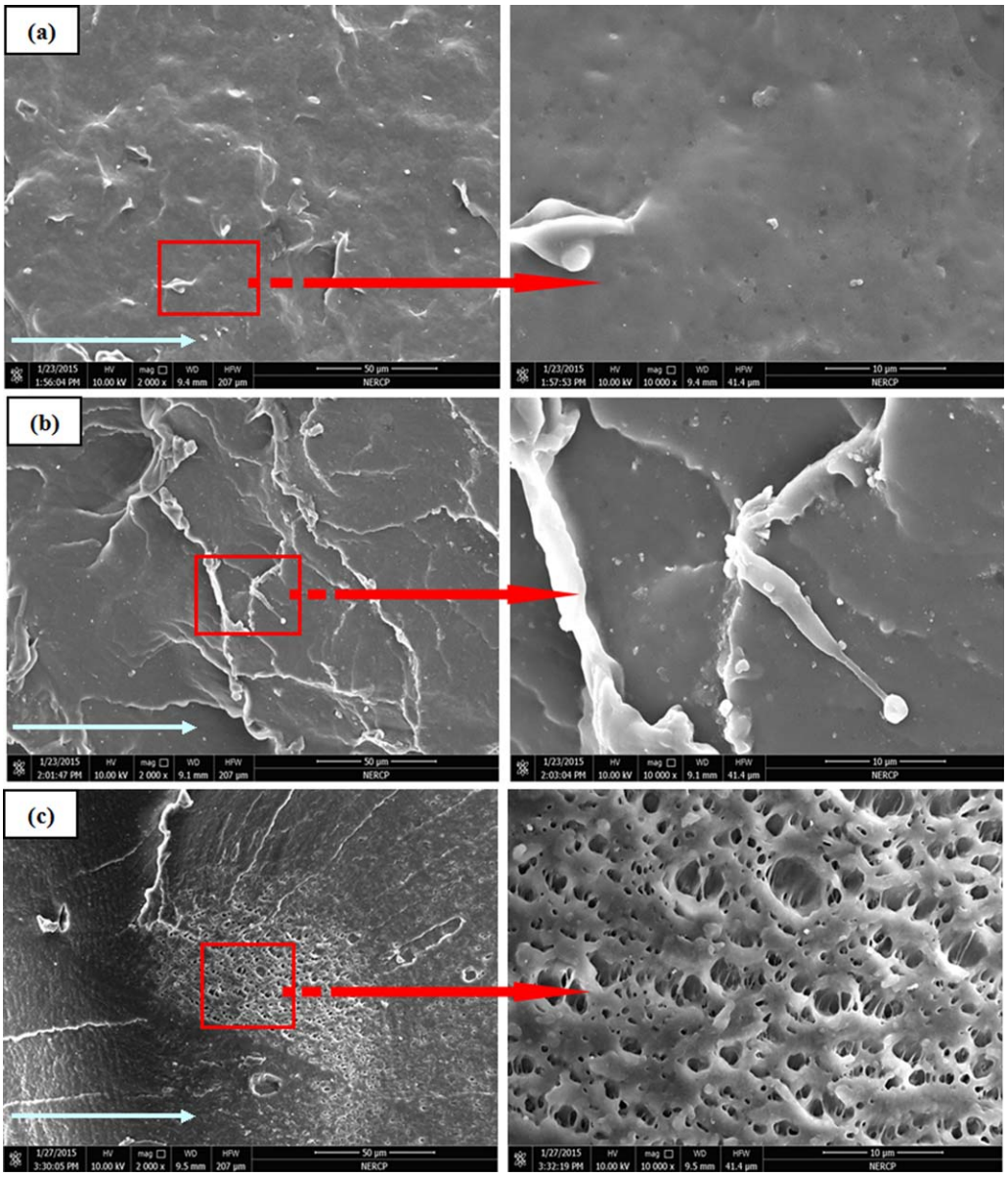

Figure 6. Impact-fractured surfaces of the PPR blends obtained at 23°C: (a) PPR, (b) PPR/TPR2088A, and (c) PPR/POE/HDPE. [Color figure can be viewed in the online issue, which is available at wileyonlinelibrary.com.]

and xylene. We found that numerous voids were dispersed in the fractured surfaces, which presented the typical droplet–matrix morphology of the PPR blends. In addition, the average size of all of the modifier particles was less than 0.5 μm, and the nanoscaled particles were more easily and uniformly dispersed in the PPR matrix. The good dispersion indicated that the rubbers presented good interfacial compatibility with the matrix. As we all know, the achievement of good compatibility during blending is crucial for promoting good interaction between the interface of the components and may improve the impact strength of the material. As shown in Figure 5(a), the particle size of TPR2088A was the smallest among these samples, and it dispersed evenly. The good dispersion and nanosized droplets of the TPR modifiers in the PPR matrix could act as stress concentrators and absorb external impact forces,[17] which were beneficial for toughening.

Additionally, the impact-fractured surfaces of the PPR composites at different temperatures (23, −10, and −30°C, respectively) are shown in Figures 6–8. The white arrows depicted in the pictures represent the crack propagation direction. As shown in Figure 6, plastic deformation (rough surface) was identified in the whole fractured surfaces at room temperature. The roughness of PPR/TPR2088A and PPR/POE/HDPE were more obvious compared with that of virgin PPR; this indicated a ductile fracture mode of the two samples at 23°C. Moreover, the obvious interface adhesion and cavitation phenomena are presented in Figure 6(c). It has been generally accepted that the existence of HDPE made the interface adhesion between POE and PPR enhanced, which played a crucial role in

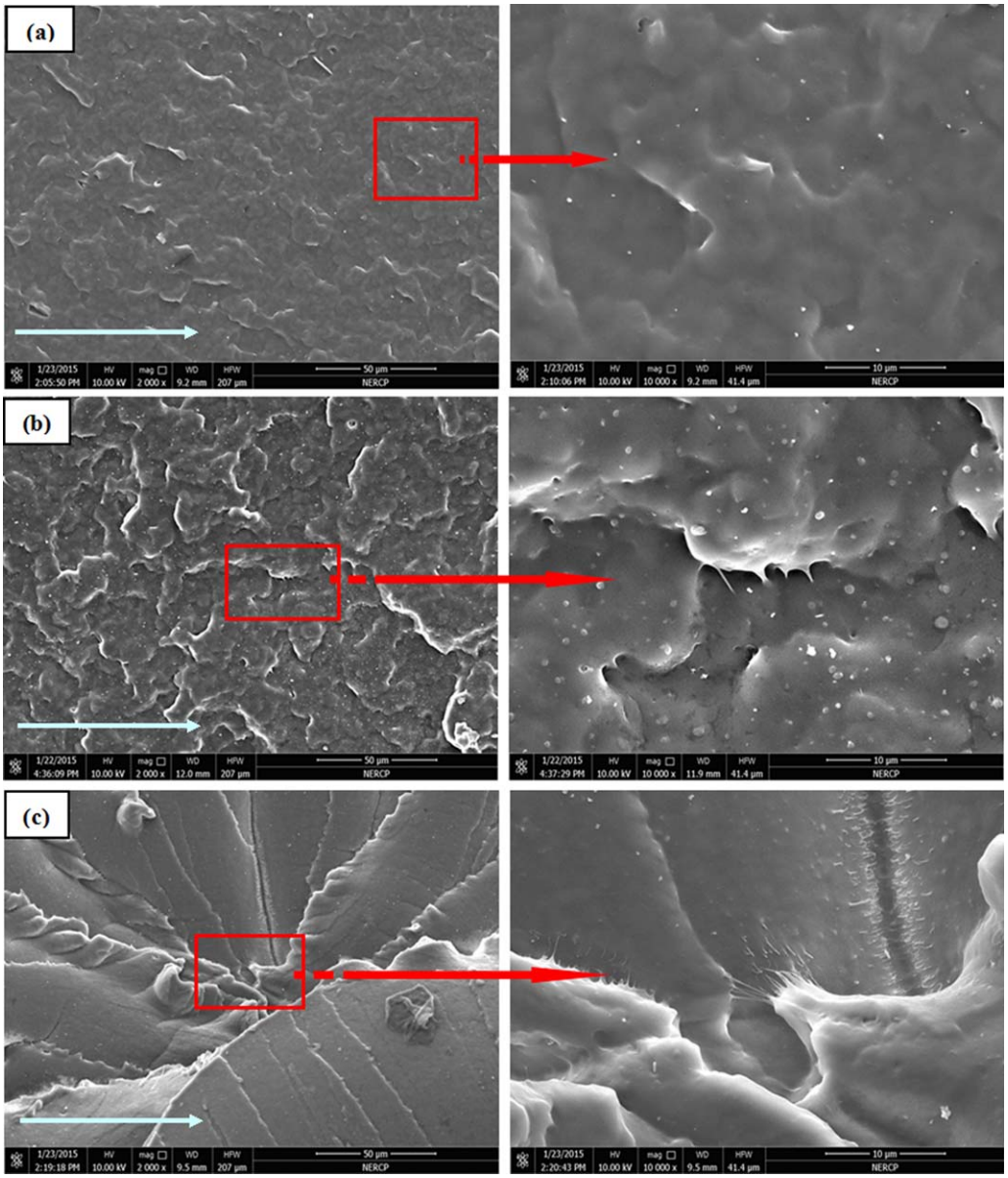

Figure 7. Impact-fractured surfaces of the PPR blends obtained at −10°C: (a) PPR, (b) PPR/TPR2088A, and (c) PPR/POE/HDPE. [Color figure can be viewed in the online issue, which is available at wileyonlinelibrary.com.]

absorbing the impact deformation energy.[38–41] It was beneficial to improve the brittle–ductile transition of rubber-toughened PPR. On the other hand, the addition of POE/HDPE promoted the shear yielding of the matrix[17,42] and resulted in the enhancement of toughness.

As shown in Figures 7 and 8, the virgin PPR exhibited an obvious brittle fracture (smooth surface) mode at both −10 and −30°C. In contrast, distinct plastic deformation was observed in the impact-fractured surfaces of PPR/TPR2088A and PPR/POE/HDPE at −10°C [Figure 7(b,c)]. Additionally, the plastic deformation of PPR/POE/HDPE was more obvious [Figure 7(c)]. This was in good agreement with the highest toughness of PPR/POE/HDPE at −10°C, as demonstrated in Figure 4(a). However, as shown in Figure 8(c), the PPR/POE/HDPE composite exhibited an obvious brittle fracture (smooth surface) mode when the temperature decreased to −30°C. On the contrary, PPR/TPR2088A with a rougher fractured surface, moderate interface adhesion, and cavitations showed the characteristics of ductile fracture; this was consistent with its highest toughness at −30°C [Figure 4(a)]. TPR2088A, with a high content of PB blocks and relatively high MFR, was more easily dispersed as small rubber particles in the matrix to better absorb the impact energy and then improved the toughness of PPR at ultralow temperatures.

Because of the previous discussions, it was reasonable to infer that both the uniform dispersion, interfacial adhesion, cavitation ability of the rubber phase, and shear yielding of the matrix were responsible for their toughness. These factors working together might transfer the composites from ductile into high ductile or even supertough materials.

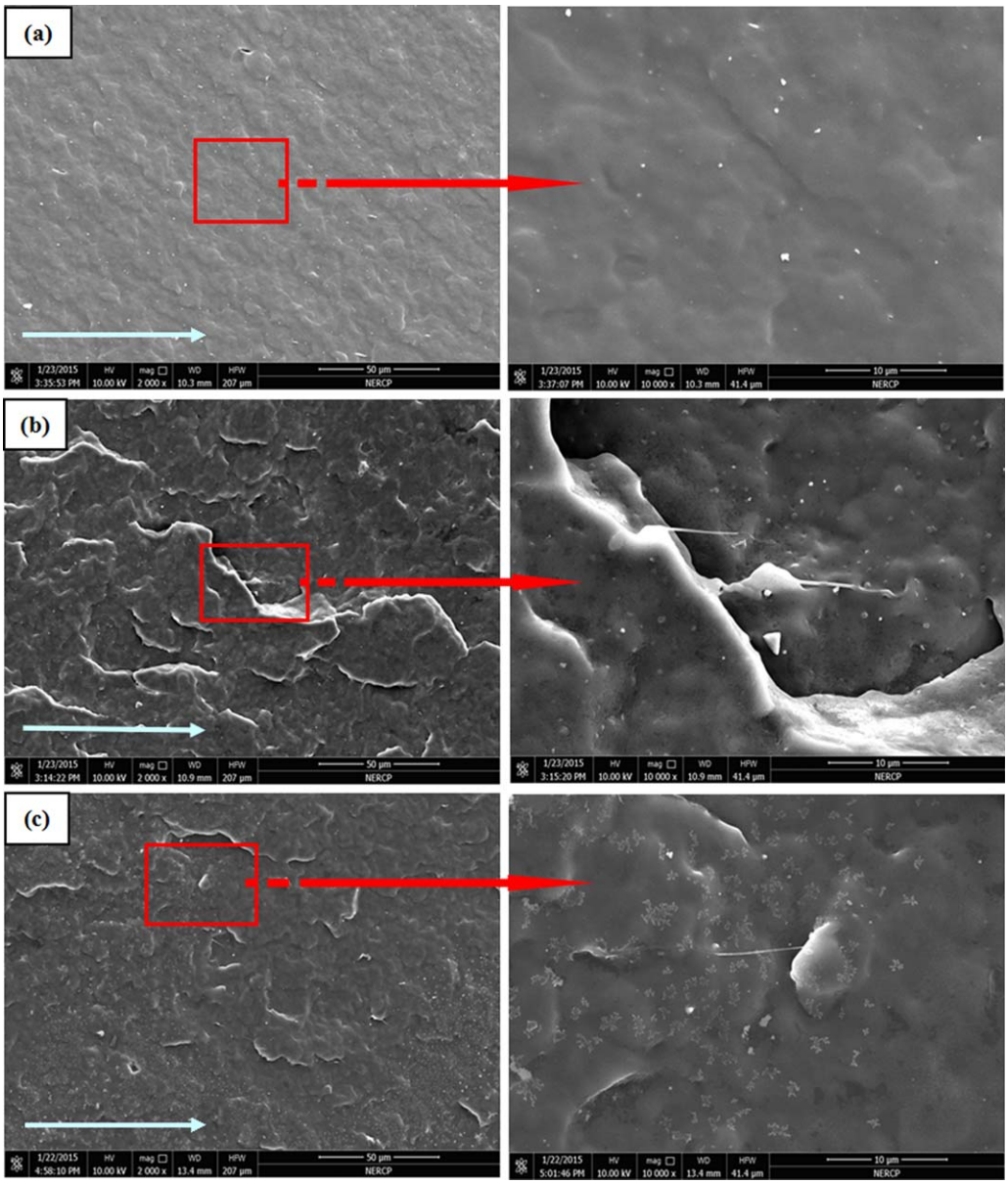

Figure 8. Impact-fractured surfaces of the PPR blends obtained at −30°C: (a) PPR, (b) PPR/TPR2088A, and (c) PPR/POE/HDPE. [Color figure can be viewed in the online issue, which is available at wileyonlinelibrary.com.]

CONCLUSIONS

Highly toughened PPR composites were prepared by the addition of different modifiers (three kinds of TPR modifiers or blends of POE/HDPE; ~10 wt %). The crystallization behaviors, dynamic mechanical properties, low-temperature performances, and microstructures of the composites were investigated. The conclusions of the study are summarized as follows:

1. The impact toughness of all of the samples showed a trend of decline with decreasing temperature, whereby the PPR/POE/HDPE ternary blends exhibited a significant enhancement in both toughness and stiffness in the temperatures interval from −10 to 23°C. In addition, the TPR modifier (type 2088A) had an excellent improvement in the toughness of PPR in the ultralow temperatures interval from −20 to −30°C with a slight decrease in the stiffness.
2. The crystallization results showed that X_C of the materials decreased after modification. The crystallinity of the PPR/POE/HDPE composite declined the most, followed by that of PPR/TPR2088A. In addition, a small amount of β crystals was induced in the PPR/2088A blends, and this could lead to the enhancement of the toughness.
3. DMA measurement confirmed that the reduction in the T_g of the matrix, the lower temperature of the elastomer phase, and the bigger I_R led to the improvement of the low-temperature toughness of the PPR composites. The T_g of PPR/TPR2088A was the lowest. In addition, the temperature of α relaxation of PPR/TPR based on TPR2088A was also the lowest. On the other hand, the I_R values of the PPR/

TPR2088A and PPR/POE/HDPE composites increased greatly. This was exactly consistent with their low-temperature performance.

4. Microstructural characterization revealed that small dispersed particle size and good compatibility played an important role in the improvement of the low-temperature impact toughness of PPR/POE/HDPE and PPR/TPR based on TPR2088A.

ACKNOWLEDGMENTS

The authors express their sincere thanks to the National Natural Science Foundation of China (contract grant number 21264004), the Industrial Research Project in Guizhou Province of China (contract grant number GZ[2013]3019), and the Functional Polymer Science and Technology Innovation Talents Team Construction in Guizhou Province of China (contract grant number [2014]4006) for their financial support.

REFERENCES

1. Fan, J. S.; Feng, J. C. *Ind. Eng. Chem. Res.* **2013**, *52*, 761.
2. Zhu, Y. L.; Feng, L.; Bai, H. W.; Wang, K.; Deng, H.; Chen, F.; Zhang, Q.; Fu, Q. *J. Appl. Polym. Sci.* **2013**, *129*, 3613.
3. Mai, J. H.; Zhang, M. Q.; Rong, M. Z.; Bárány, T.; Ruan, W. H. *Express Polym. Lett.* **2012**, *6*, 739.
4. Zhang, Z. S.; Wang, C. G.; Zhang, J. P.; Mai, K. C. *J. Therm. Anal. Calorim.* **2012**, *109*, 1587.
5. Papageorgiou, D. G.; Vourlias, G.; Bikiaris, D. N.; Chrissafis, K. *Macromol. Mater. Eng.* **2014**, *299*, 707.
6. Papageorgiou, D. G.; Vourlias, G.; Bikiaris, D. N.; Chrissafis, K. *Macromol. Chem. Phys.* **2014**, *215*, 839.
7. Li, M.; Li, G.; Jiang, J.; Tao, Y.; Mai, K. C. *Compos. Sci. Technol.* **2013**, *81*, 30.
8. Liu, B. B.; Shangguan, Y. G.; Song, Y. H.; Zheng, Q. *J. Appl. Polym. Sci.* **2013**, *129*, 973.
9. Liu, B. B.; Shangguan, Y. G.; Zheng, Q. *Chin. J. Polym. Sci.* **2012**, *30*, 853.
10. Leng, J. H.; Liu, H.; He, B. B.; Yang, B.; Chen, X.; Qin, Q. Q. *Chin. J. Polym. Sci.* **2013**, *31*, 1563.
11. Luo, F.; Zhu, Y. L.; Wang, K.; Deng, H.; Chen, F.; Zhang, Q.; Fu, Q. *Polymer* **2012**, *53*, 4861.
12. Li, M.; Li, G.; Zhang, Z. S.; Dai, X.; Mai, K. C. *Thermochim. Acta* **2014**, *598*, 36.
13. Yu, L.; Wu, T.; Chen, T.; Yang, F.; Xiang, M. *Thermochim. Acta* **2014**, *578*, 43.
14. Ding, J.; Ding, X. J.; Xu, R. W.; Yu, D. S. *J. Macromol. Sci. Phys.* **2005**, *44*, 303.
15. Tang, W. H.; Tang, J.; Yuan, H. L.; Jin, R. G. *J. Appl. Polym. Sci.* **2011**, *122*, 461.
16. Abreu, F. O. M. S.; Forte, M. M. C.; Liberman, S. A. *J. Appl. Polym. Sci.* **2005**, *95*, 254.
17. Tang, J.; Tang, W. H.; Yuan, H. L.; Jin, R. G. *J. Appl. Polym. Sci.* **2010**, *115*, 190.
18. Sanft, P.; Francis, L. F.; Davidson, J. H. *J. Sol. Energy Eng.* **2006**, *128*, 251.
19. Ou, C. F. *Eur. Polym. J.* **2002**, *38*, 467.
20. Houshyar, S.; Shanks, R. A.; Hodzic, A. *Polym. Test* **2005**, *24*, 257.
21. Li, J. X.; Cheung, W. L.; Jia, D. M. *Polymer* **1999**, *40*, 1219.
22. Turner-Jones, A.; Aizlewood, J. M.; Beckett, D. R. *Macromol. Chem. Phys.* **1964**, *75*, 134.
23. Su, R.; Li, Z.; Bai, H. W.; Wang, K.; Zhang, Q.; Fu, Q.; Zhang, Z. J.; Men, Y. F. *Polymer* **2011**, *52*, 3655.
24. Bucknall, C. B. *Polymer* **1978**, *27*, 121.
25. Chen, Y. H.; Ye, L. *J. Appl. Polym. Sci.* **2011**, *121*, 1013.
26. Chen, H. B.; Karger-Kocsis, J.; Wu, J. S.; Varga, J. *Polymer* **2002**, *43*, 6505.
27. Xu, H.; Cebe, P. *Macromolecules* **2004**, *37*, 2797.
28. Song, M. *J. Appl. Polym. Sci.* **2001**, *81*, 2779.
29. Boyd, R. H. *Polymer* **1985**, *26*, 323.
30. Read, B. E. *Polymer* **1989**, *30*, 1439.
31. Chen, J. W.; Dai, J.; Yang, J. H.; Huang, T.; Zhang, N.; Wang, Y. *J. Mater. Res.* **2013**, *28*, 3100.
32. Jafari, S. H.; Gupta, A. K. *J. Appl. Polym. Sci.* **2000**, *78*, 962.
33. Grein, C.; Bernreitner, K.; Gahleitner, M. *J. Appl. Polym. Sci.* **2004**, *93*, 1854.
34. Li, S. C.; Hu, H. L.; Zeng, W. *Polym. Plast. Technol. Eng.* **2012**, *51*, 744.
35. Li, Y. M.; Wei, G. X.; Sue, H. J. *J. Mater. Sci.* **2002**, *37*, 2447.
36. Ardakani, F.; Jahani, Y.; Morshedian, J. *Polym. Eng. Sci.* **2014**, *54*, 1747.
37. Bull, A. L.; Holden, G. *J. Elastomers Plast.* **1977**, *9*, 281.
38. Lin, Y.; Chen, H. B.; Chan, C. M.; Wu, J. S. *Macromolecules* **2008**, *41*, 9204.
39. Geng, C. Z.; Yang, G. H.; Bai, H. W.; Li, Y. H.; Fu, Q.; Deng, H. *J. Supercrit. Fluids* **2014**, *87*, 83.
40. Vander Wal, A.; Gaymans, R. *J. Polymer* **1999**, *40*, 6067.
41. Starke, J. U.; Michler, G. H.; Grellmann, W.; Seidler, S.; Gahleitner, M.; Fiebig, J.; Nezbedova, E. *Polymer* **1998**, *39*, 75.
42. Jang, B. Z.; Uhlmann, D. R.; Vander Sande, J. B. *Polym. Eng. Sci.* **1985**, *25*, 98.